Logjams and channel morphology influence sediment storage, transformation of organic matter, and carbon storage within mountain stream corridors

Nicholas A. Sutfin[1,2*], Ellen Wohl[1], Timothy Fegel[3], Laurel Lynch[4]

[1]*Department of Geosciences, Colorado State University, Fort Collins, CO 80523-1482*
[2]*Integrated Water, Atmosphere, and Ecosystem Education and Research Program, Colorado State University*
[3]*Rocky Mountain Research Station, United States Forest Service, Fort Collins, CO 80526*
[4] *Department of Soil and Water Systems, University of Idaho, Moscow, ID 83844*
[*]Corresponding author current affiliation: Department *of Earth, Planetary, and Environmental Sciences, Case Western Reserve University, Cleveland, OH 44106*

Key Points

- Less confined valleys store more carbon in floodplain fine sediment and large wood compared to more confined valley segments
- Channels with single thread planforms store more carbon than more complex systems with multiple channels of flow across the valley bottom
- Logjam abundance appears to limit fine sediment depth and promote transformation of organic matter in complex multithread reaches

Abstract

The flow of organic matter (OM) along rivers and its retention within floodplains are fundamental to the function of aquatic and riparian ecosystems and are significant components of terrestrial carbon storage and budgets. Carbon storage and ecosystem processing of OM largely depends upon hydrogeomorphic characteristics of streams and valleys. To examine the role of channel complexity on carbon dynamics in mountain streams, we (1) quantify organic carbon (OC) storage in sediment and wood along 24 forested stream reaches in the Rocky Mountains of CO, U.S.A., (2) employ six years of logjam surveys and examine related morphological factors that regulate sediment and carbon storage, and (3) utilize fluorescence spectroscopy to examine how the composition of OM in surface water and floodplain soil leachates is influenced by valley and channel morphology. We find that lower-gradient stream reaches in unconfined valley segments at high elevations store more OC per area than higher-gradient reaches in more confined valleys, and those at lower elevations. We find that limited storage of fine sediment and

increased mineralization of OC in multithread channel reaches decrease storage per area compared to simpler single-thread channel reaches. Results suggest that the positive feedbacks between channel complexity and persistent channel-spanning logjams that force multiple channels to flow across valley bottoms limit the aggradation of floodplain fine sediment, and promote hotspots for the transformation of OM. These multithread hotspots likely increase ecosystem productivity and ecosystem services by filtering dissolved organic carbon with potential to decrease contaminants associated with organic matter from surface water.

Introduction

Instream wood and logjams along river corridors have been linked to increases in retention of floodplain sediment and organic matter (OM), the dynamics of which are important for the integrated function of ecosystems, soils, and water resources. It is well recognized that large instream wood facilitates heterogeneity along rivers (Wohl, 2014), diverse aquatic habitats (Gurnell et al., 2000), increased biodiversity (Fetherston et al., 1995; Ward et al., 1999), feedbacks that facilitate the deposition and storage of floodplain sediment (Montgomery & Abbe, 2006; Collins et al., 2012; Wohl & Scott, 2017), and increases in the storage of organic carbon (OC) (Hyatt & Naiman, 2001; Guyette et al., 2002; Wohl et al., 2012; Beckman & Wohl, 2014; N. A. Sutfin & Wohl, 2017; Scott & Wohl, 2018; K. B. Lininger et al., 2019). Allochthonous organic matter OM inputs and dynamics in headwater streams provide the foundation of food webs crucial for fisheries and autochthonous primary production in larger rivers downstream (Vannote et al., 1980; Chapin et al., 2011), and can greatly influence the fate and transport of contaminants in sediment, soil, and surface water (Huang et al., 2003; Borch et al., 2010). In addition to the ecosystem services mentioned above, smaller streams can facilitate

OC reservoirs for terrestrial carbon budgets. Because smaller order streams constitute a large majority (~95%) of river length globally (Downing et al., 2012), these systems are also important when considering carbon (C) reservoirs in the terrestrial C cycle. We refer, herein, to "OC" when discussing storage reservoirs of organic carbon (Mg C ha^{-1}) and "OM" when discussing specific sources of OC and the decomposition or transformation of those sources by microbial communities and aquatic invertebrates.

The highest uncertainty in annual exchanges of C between the atmosphere, surface ocean, and land surface occurs within terrestrial reservoirs (Gregory et al., 2009; Ballantyne et al., 2012), which include rivers and floodplains. Past research has shown that water bodies and rivers play a significant role in terrestrial C budgets through release to the atmosphere, delivery to the oceans (Cole et al., 2007; Battin et al., 2009; Tranvik et al., 2009; Aufdenkampe et al., 2011; Galy et al., 2015), and substantial storage along river corridors (Thomas Hoffmann et al., 2009; Wohl et al., 2012; D'Elia et al., 2017; N. A. Sutfin et al., 2016; N. A. Sutfin & Wohl, 2017). Total C storage among terrestrial reservoirs is highest in soils (Falkowski et al., 2000), which have the potential to store a significant amount of organic carbon (OC) at depth along river corridors (Hoffmann et al., 2009; Sutfin et al., 2016; D'Elia et al., 2017; Omengo et al., 2018; Lininger & Wohl, 2019).

Determining whether OC retention within floodplains constitutes long-term C storage requires considering (1) the duration for floodplain sediment to remain in storage prior to downstream transportation, and (2) potential for OM decomposition and mineralization to the atmosphere. Because geomorphic response to flood conditions regulating the former (N. A. Sutfin & Wohl, 2019) and biogeochemical processes regulating the latter depend on hydrologic connectivity (Vannote et al., 1980; Battin et al., 2008; Lynch et al., 2019) the potential for OC

81 storage along river corridors is highly sensitive to changes in hydrological conditions and flow
82 regimes. Recent work examining floodplain sediment residence times in the Colorado Front
83 Range, USA – which examined some of the same study reaches included in the work presented
84 here - found that valley and channel form may play a significant role in the degree to which
85 sediment storage responds to shifts in hydrologic regime (N. A. Sutfin & Wohl, 2019). Valley
86 confinement and overbank stream power were the strongest predictors for floodplain sediment
87 residence time. Thus, the influence of hydrology on sediment dynamics and associated carbon
88 storage within river corridors regulated by factors that influence valley and channel geometry.
89 Biophysical factors that influence channel form and hydrologic connectivity include in-
90 stream wood, logjams, beavers, vegetation, valley width and confinement, and hydrologic flow
91 and sediment regimes, which together control the variability of irregularities in river channel
92 morphology (Polvi & Wohl, 2013) and channel complexity (Livers & Wohl, 2016). We refer
93 herein to the presence and variability of diverse channel geometry, including planform and
94 bedforms, as 'channel complexity', where greater channel complexity equates to increased
95 spatial variability in channel geometry (Livers & Wohl, 2016). Increased channel complexity is
96 more common along headwater streams as a result of limited human impact and increased
97 presence of biotic drivers (large wood, beavers) of channel morphology in the study area (Polvi
98 & Wohl, 2013; Beckman & Wohl, 2014). As a result, limited studies have suggested (Wohl et
99 al., 2012) and a review of previous work has posited that complex headwater streams have
100 higher capacity to store OC (N. A. Sutfin et al., 2016).
101 Floodplains along 1st, 2nd, & 3rd order mountainous headwater streams have higher soil
102 organic carbon (SOC) content than adjacent uplands (Wohl et al., 2012; N. A. Sutfin & Wohl,
103 2017), and can store more carbon per area than higher-order lowland rivers (N. A. Sutfin et al.,

2016). Complex channel segments have been observed to store more C per area along mountain river corridors than simpler river segments (Wohl et al., 2012), and it has been posited that these complex beads serve as significant reservoirs for OC storage (Wohl, Lininger, et al., 2017). However, past research posited that more complex channels are hotspots for OM decomposition because they increase water residence times (Gooseff et al., 2007) and provide greater opportunities for microbial metabolism (Battin et al., 2008). Furthermore, recent work shows that the composition of organic matter flowing through complex channel segments is more molecularly diverse than that of single-thread channels; these differences become increasingly pronounced as seasonal declines in flow reduce hydrologic connectivity across the floodplain (Lynch, et al., 2019).

The objectives of the research presented here are to (1) quantify differences in OC storage per area along valley segments with varying channel and valley geometry, (2) examine potential hydrogeomorphic mechanisms for those potential differences in storage, and (3) examine longitudinal trends in the composition of organic matter as it cycles through surface waters and adjacent floodplains. To do this, we surveyed 24 relatively undisturbed study reaches with similar geology, climate, and vegetation type along the tributaries and main stem of four streams that flow into the South Platte River in northern Colorado. Within these study reaches we examined biophysical controls on floodplain sediment dynamics and microbial transformation of organic matter along mountain stream corridors.

Study Area

The underlying lithologic core of the Colorado Front Range (CFR) is composed of Precambrian gneiss, schist, granite and other igneous rocks primarily of intrusive origin (Braddock & Cole, 1990). Irregular spacing of bedrock jointing facilitates longitudinal

variability in the relative confinement of stream valleys, such that broader valleys commonly coexist with more closely spaced bedrock joints and strath terraces along otherwise confined, narrower valleys (Wohl, 2008). On the eastern side of the CFR, knickpoints at approximately 2,000 m in elevation mark the transition of broader glaciated valleys where streams incised through sedimentary rocks at the eastern margin of the Precambrian core (Anderson et al., 2006). Pleistocene terminal moraines extend eastward down-valley to elevations of approximately 2,300 to 2,500 m.

Vegetation in the study area reflect changes across the ecotone from montane to subalpine forests in the CFR. At 1,830-m elevation, grassland steppe vegetation transitions into montane forest, which is dominated by ponderosa pine (*Pinus ponderosa var. scopulorum*) and Douglas-fir (*Pseudotsuga menziesii*) extending to ~2,750 m. The montane zone receives ~50 cm of rainfall annually (Barry, 1973; Birkeland et al., 2003) and experiences relatively frequent and low severity ground fires approximately every 30-100 years. Forests in the subalpine zone, extending from ~2,750 to 3,400 m, are dominated by subalpine fir (*Abies lasiocarpa*), lodgepole pine (*Pinus contorta*), limber pine (*Pinus flexilis*), Engelmann spruce (*Picea englemannii*), and aspen (*Populus tremuloides*) (Veblen & Donnegan, 2005). Large stand-replacing fires occur on average every 500 years in the subalpine zone, where annual average precipitation is ~77 cm and increases to ~100 cm in the alpine zone (Barry, 1973; Birkeland et al., 2003). The alpine zone above 3,400 m elevation is defined by alpine tundra, which has limited forest with krummholz conifers of the same species that populate the subalpine zone. Vegetation within the riparian zone typically corresponds to that of respective upland vegetation with additions of blue spruce (*Picea pungens*), and in the subalpine zone Douglas fir, Engelmann spruce, and aspen are abundant. Willow (*Salix* spp.), sedges (*Carex* spp.), and river birch (*Betula fontinalis*) are present

where evidence of contemporary or relict beaver activity is present (Veblen & Donnegan, 2005; Polvi et al., 2011).

Snowmelt typically results in a single annual hydrograph peak during late May or early June along streams in the CFR, with some caveats along an elevational gradient. Paleoflood indicators and estimates of flood magnitudes (McCain & Shroba, 1979; Jarrett, 1990) suggest that increased intensity of large convective thunderstorms disproportionately influence stream discharges at elevations below 2,300 m, sometimes resulting in secondary peak flows that exceed the snowmelt-dominated peak (Jarrett, 1990). In addition, differences in glaciation, forest type, fire frequency, and resulting hydrologic flow paths likely influence the hydrogeomorphic impact of these convective storms, which have been shown to reduce floodplain sediment residence times at lower elevations (N. A. Sutfin & Wohl, 2019).

Channel morphology and OC retention in the CFR – where streams are dominated by cobble to boulder substrate and vary from cascade, plane bed, step-pool, pool-riffle bed morphology (Livers & Wohl, 2015) – are influenced by large wood and logjams. Transitional morphological states in channel form also occur in the study area, particularly where land-use has altered wood regimes (Livers et al., 2018). Variability in forest age and valley geometry are reflected in the longitudinal variability of instream wood loads and spacing of channel spanning logjams (Wohl and Cadol, 2011). Instream wood, irregularities in channel boundaries, diversity and spacing of pool-riffle and step-pool sequences, and the presence of side channels or multiple channels of flow across the valley bottom contribute to what we refer to herein as ‘channel complexity’ (Livers & Wohl, 2016). While OC storage in pool sediments upstream of logjams is positively correlated with the volume of instream wood, OC stored as instream wood exceeds storage in pool sediments (Beckman & Wohl, 2014). Fine sediment deposits in floodplains are

dominated by sand and contain substantially higher OC content than adjacent uplands (N. A. Sutfin & Wohl, 2017). OC storage per area in the CFR is greatest within wider valley segments and where channel complexity is highest as a result of logjam-forced multithread channels (Wohl et al., 2012). The largest OC reservoir in multithread channels was large downed wood on the floodplain, but a small number of study reaches limit the statistical power of prior observations.

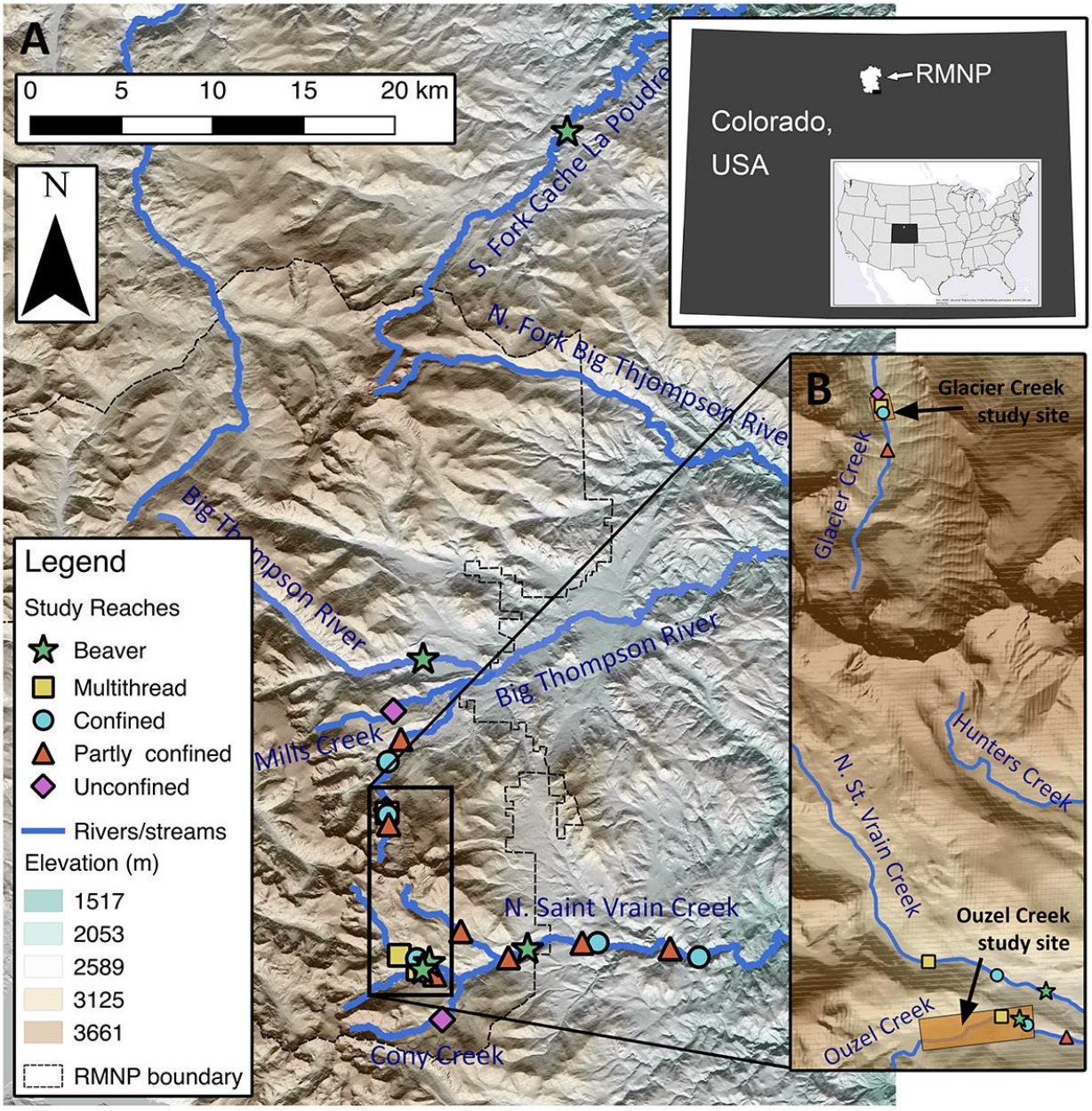

Figure 1. Map of the study area along the Colorado Front Range of the Rocky Mountains, U.S. Twenty-four study reaches representing five different valley types (A) are indicated in the legend. Orange rectangles identify intensive study segments that transition between single thread-multithread-single thread reaches on Glacier and Ouzel Creeks (B). At these intensive study sites, organic matter composition was examined along transitions in valley confinement using fluorescence spectroscopy. Logjam surveys were conducted in the N. Saint Vrain Creek Basin upstream of the RMNP boundary.

Methods

Study reaches

Located within and around Rocky Mountain National Park and the Arapaho and Roosevelt National Forests, 24 study reaches were surveyed in the subalpine and the montane zones of nested tributaries within North Saint Vrain Creek (NSV), Glacier Creek (GCK), South Fork of the Poudre River (SFP), and the Big Thompson River (BTR) watersheds (Figure 1). Smaller tributaries examined include Ouzel, Cony, Hunters, and Mills Creeks. Bedrock gravel-bed study reaches examined here include step-pool, pool-riffle, and plane bed morphologies (Montgomery & Buffington, 1997; Livers & Wohl, 2015). Step-pool morphologies include boulder and logjam-forced steps.

We characterize study reaches by relative channel complexity as described above and a valley confinement ratio (C_r), calculated as the stream channel width divided by the valley width. Reaches with $C_r > 0.5$ are classified as confined (CF), those with a ratio between 0.5 and 0.24 as partly confined (PC), and those with $C_r < 0.24$ as relatively unconfined valleys (UC; Table 1). We classify study reaches with a range of valley confinement ratios that have field evidence of exposed or buried beaver dams and ponds, beaver-dug canals for water diversion, beaver lodges, beaver mounds and slides, and beaver chewed trees as abandoned or active beaver meadows (AB) (Ives, 1942; Polvi & Wohl, 2012, 2013). In old-growth forests of the Colorado Front Range (>200 years old) trees are large enough to create channel-spanning logjams within unconfined

valleys. Where logjams persist for a year or more, flow can be diverted around the logjams, resulting in secondary channels and sometimes multiple channels of flow across the valley bottom. We refer to these complex channel segments, where evidence of beavers is not present, as multithread channels (MT) and include them as a class within our study reaches.

Table 1. Physical attributes of the 24 study reaches. Reaches are located along North St. Vrain Creek (NSV) and tributaries, Cony, Ouzel, and Hunters Creeks; the Big Thompson River (BTR) and tributary Mills Creek; Glacier Creek; and the South Fork Cache La Poudre River (SFP).

Stream	Study Reach	Valley type	Valley width (m)	Channel width (m)	Valley confinement (m/m)	Gravimetric soil moisture content (%)	Stream Gradient (%)	Elevation (m)	Drainage Area (km^2)
NSV	CF1	Confined	18	13.0	0.73	16	0.032	2385	97.7
Ouzel	CF2	Confined	9	5.3	0.55	35	0.095	2971	10.7
Glacier	CF3	Confined	12	8.5	0.32	34	0.13	2845	21.0
NSV	CF4	Confined	11	6.2	0.58	38	0.085	2951	17.9
NSV	CF5	Confined	19	14.1	0.74	20	0.026	2162	205.1
Glacier	CF7	Confined	10	5.6	0.50	42	0.09	3071	9.7
NSV	PC1	Partly confined	33	17.1	0.45	21	0.037	2420	96.4
Ouzel	PC2	Partly confined	14	5.1	0.34	38	0.063	2927	11.1
Glacier	PC3	Partly confined	33	8.5	0.26	25	0.027	2701	33.2
Hunters	PC4	Partly confined	15	3.7	0.24	30	0.069	3013	10.1
NSV	PC5	Partly confined	27	12.7	0.45	23	0.023	2226	200.5
NSV	PC7	Partly confined	43	14.5	0.31	48	0.016	2573	77.4
Glacier	PC6	Partly confined	14	4.2	0.28	34	0.02	3118	7.1
Cony	UC1	Unconfined	26	5.6	0.21	58	0.028	3054	12.7
Glacier	UC2	Unconfined	32	5.1	0.15	54	0.013	3053	10.3
Mills	UC3	Unconfined	47	7.8	0.10	41	0.01	2797	3.0
NSV	AB1	Beaver	67	6.8	0.10	55	0.037	2901	19.1
Ouzel	AB2	Beaver	43	7.0	0.13	65	0.04	2978	10.6
NSV	AB4	Beaver	247	14.1	0.05	40	0.012	2547	82.2
BTR	AB5	Beaver	180	17.3	0.09	29	0.006	2462	93.7
SFP	AB6	Beaver	77	10.6	0.13	25	0.011	2410	180.6
NSV	MT1	Multithread	61	6.5	0.10	44	0.063	3035	14.8
Glacier	MT2	Multithread	34	6.7	0.18	39	0.03	3068	9.8
Ouzel	MT3	Multithread	53	5.2	0.10	53	0.033	2990	10.5

Field surveys and soil sampling for carbon storage

Study reaches were characterized by 11 transects spaced approximately one bankfull width apart and oriented orthogonally to the down-valley direction. Field surveys were

conducted and sediment samples were collected in the summer months of 2012, 2013, and 2014. A stadia rod and a laser rangefinder with 10-cm accuracy (Laser Technologies®, TruPulse 360B) were used to survey topography along each transect at breaks in slope and other points of interest (e.g., changes in grain size, transitions in vegetation type) with a maximum spacing of ~11 m between survey points. Approximate bankfull channel width was determined between points along each transect using the height of depositional features including point bars and changes in vegetation as primary bankfull indicators. The stream gradient was measured by surveying the estimated bankfull stage on the banks along the length of each study reach including an additional channel width at the upstream and downstream end.

The depth of the underlying floodplain fine sediment (<2 mm) was measured by inserting a 1-cm diameter soil probe until refusal at bedrock or coarser pebble and cobble material. The optimal number of samples to be collected at each study reach was selected as the result of intensive sampling and bootstrap analysis, which indicated that the bias in estimates of reach-average organic carbon content along each study reach was reduced at approximately 10-11 sampling locations (N. A. Sutfin & Wohl, 2017). Soil sampling locations were selected through systematic random sampling at a distance identified through a random number generator using increments of 1 m along each transect, which resulted in 273 sampling locations. Volumetric samples of organic matter in the O-horizon were collected as a single sample at each sampling location using a cylindrical sampling tube. A ~7 cm diameter stainless steel hand auger was used to sample sediment at increments of 15-cm depth until refusal at bedrock or material exceeded ~2 mm in diameter. Auger length prevented sample collection at depths greater than 180 cm, which occurred at three sampling locations. Twenty-one volumetric soil samples were collected in small trenches excavated along the floodplain to estimate bulk density by inserting a 7-cm

diameter soil sampling tube horizontally and centered at ~5, 15, and 45 cm depth where roots did not interrupt sampling (Supplemental Table S1). Dominant vegetation and primary tree types were recorded along each reach and noted at survey points along each transect to verify typical vegetation type, but were not used in statistical analysis.

Contributing drainage area for each study reach was calculated using 10-m resolution USGS digital elevation models (DEMs) in ESRI ArcMap. The elevation of each reach was taken as the elevation from the DEMs at the downstream transect along each study reach. Stream gradient was calculated as the slope of the linear regression line fit to all surveyed stream gradient points described above.

Carbon storage as floodplain large wood

The length and diameter of downed floodplain wood greater than 1-m in length and 10-cm in diameter were measured and wood volumes were calculated as the volume of a cylinder using the average diameter of the two end measurements. The mass of C stored in each large wood piece was estimated using an average density of 400 kg m^{-3} for softwood species in the area (Glass & Zelinka, 2004) and assuming 50% C by mass.

Analysis of organic carbon content

A total of 660 mineral soil samples were collected and frozen until analysis for OC content by the Colorado State University Soil and Water Testing Laboratory. A subset of each sample was dried for 48 hours at 60ºC, then ground and analyzed for total C and N by dry combustion (LECO 1000 CHN analyzer, LECO Corporation, St. Joseph, MI, USA). Each sample was then analyzed for inorganic carbon (CO_3-C) by treating the sample with 0.4 N HCl and

263 measuring the CO_2 loss gravimetrically. Soil organic carbon (SOC) content by weight was
264 calculated as total carbon minus inorganic carbon. The gravimetric soil moisture content was
265 determined as the difference between the mass of field-moist soil and sediment dried at 105°C
266 for 24 hours. A total of 281 O-horizon samples consisting of recognizable plant material (< 6
267 mm diameter, including litter and needles), and duff (unrecognizable and fragmented material
268 between the litter and mineral soil layers, FIA, 2019) were dried at 105°C for 24 hours. OC
269 content of the O-horizon was estimated as 50% of the mass lost through loss on ignition at 550°C
270 after 24 hours.

271 *Carbon storage calculations*

272 Measured depths of fine sediment, bulk density measurements, and SOC content were
273 used to estimate floodplain sediment carbon storage per area along each study reach. The volume
274 of floodplain fine sediment was calculated by generating triangular irregular networks (TINs)
275 using ESRI ArcMap. The volume of sediment was multiplied by the average bulk density across
276 study reaches (ρ_b = 0.9 ± 0.24 g cm^{-3}), as representative of floodplain sediment in the study area
277 (Supplemental Table S1), to estimate the mass of floodplain sediment along each study reach.
278 Bulk density and OC content did not vary consistently with depth or significantly across channel
279 types, and buried lenses of organic-rich sediment were common (N. A. Sutfin & Wohl, 2017).
280 Mean OC content of samples averaged across all depths at each sampling location were therefore
281 used to estimate OC storage at each reach. The total mass of sediment along each study reach
282 was multiplied by the mean gravimetric soil OC content along each reach to calculate the total
283 mass of OC storage in floodplain sediment.

284 Depth, bulk density, and OC content of the combined litter and duff layer measured at
285 each reach was used to estimate organic carbon storage in this reservoir. Average depth of the

combined litter and duff layer was multiplied by the floodplain surface area – generated from TINs as described above – to estimate the volume of the O-horizon at each study reach. The product of the volume of litter and duff and its average bulk density were used to calculate the mass of sediment, which was multiplied by the average OC content to estimate the mass of OC storage for each study reach.

Total mass of OC in all floodplain reservoirs (i.e., sediment, litter and duff, and wood) was divided by the surface area of each TIN to estimate total OC storage per area along each study reach.

Instream logjam surveys

We utilized an ongoing absence-presence survey of logjams in the North St. Vrain Creek watershed to examine relationships between logjams and the depth of floodplain fine sediment. The number of instream logjams was monitored and recorded annually over a six-year period from 2010 to 2015 along nine study reaches in the North Saint Vrain Creek watershed (Supplemental Table S2). Logjams locations were recorded using a handheld GPS unit upstream of the Pleistocene terminal moraine located at approximately 2,500 m elevation. Logjams that fell within the ESRI ArcMap shapefile extent of the surveyed study reach, plus one channel width up and down valley of each study reach, were summed for each year. We estimate mean floodplain fine sediment depth by dividing the floodplain sediment volume by the surface area of the study reach. Because floodplain fine sediment depth among study reaches is significantly different between confined and partly confined reaches ($p < 0.05$), we account for varying degrees of confinement by standardizing sediment depth by the mean valley width. In addition to the six-year average number of logjams, we examine potential influence on the depth of

floodplain sediment by considering other variables including drainage area, elevation, and stream gradient using stepwise multiple linear regression.

Analysis of stream and soil water chemistry

Surface water and soil samples were collected along two intensive study segments capturing single thread-multithread-single thread downstream transitions on Ouzel Creek (August 18, 2014) and Glacier Creek (August 19, 2014) to examine relative changes in the composition of dissolved organic matter upstream and downstream of multithread reaches. The Ouzel Creek intensive study site is ~1,600 m long, with an upstream confined reach of ~200 m, a multithread reach of ~1,200 m, and a downstream confined study reach of ~200 m. The Glacier Creek intensive study sites is ~195 m long, with upper confined, middle multithread, and lower partly confined study reaches all ~65 m in length. Transects were located near both the upstream and downstream extent of each of the three subreaches, resulting in six transects that define the two intensive paired sites. Soil core sampling locations were selected in the same random process described above on both channel banks of each transect where the bank did not consist of bedrock. An additional sample location was randomly selected along an island of each transect within the multithread sub-reaches. Organic material composed of duff and litter was removed and measured, and fine mineral sediment was sampled where present (some locations were located on bedrock, boulders, or were composed entirely of duff and litter) in increments of ~15 cm until refusal at bedrock or gravel. The number of soil samples collected at each site varied by the depth of available sediment/mineral soil, which was sometimes zero (Supplemental Table S3). Paired surface-water samples were collected at one location along each confined and partly confined transect, and within the main stem and at least one side channel along the multithread reaches (totaling 8 samples for Glacier Creek and 9 samples for Ouzel). Acid-washed Nalgene®

HDPE bottles were rinsed six times with water before a sample was collected. All samples were immediately taken back to the lab where soil samples were frozen until further analysis and water samples were processed immediately.

Surface-water samples were filtered through pre-combusted (400°C) 0.7 μm glass fiber filters (Whatman GF/F) within six hours of collection and acidified to pH 3. Dissolved organic carbon (DOC) and total dissolved nitrogen (TDN) were determined by high-temperature combustion catalytic oxidation using a Shimadzu TOC-V_{CPN} analyzer equipped with a sparging method for non-purgeable organic carbon (NPOC, hereafter referred to as DOC) (Shimadzu Corporation Columbia, MD). Detection limits for DOC and TDN were 50 μg L^{-1}.

We weighed 5 g of floodplain soil and 10 mL of nanopure water (< 18.2 MΩ-cm) into sterile 50 mL centrifuge tubes fit with 0.45 μm spin filters. Samples were centrifuged for 20 minutes at 3,400 rpm and 24°C. Nutrient (NO_3^- and NH_4^+) concentrations of subsurface floodplain leachates were determined by ion chromatography via electrical conductivity detection, using an AS12A Anion-Exchange column for anions and CS12A columns for cations (Dionex Corp, Sunnyvale, CA). Detection limits for NO_3^- and NH_4^+ were 10 μg L^{-1}. DOC and TDN concentrations for subsurface floodplain leachates were determined using a Shimadzu TOC-V_{CPN} analyzer, as above.

UV-Fluorescence properties of surface-water and floodplain soil water leachates were measured using an Aqualog spectrofluorometer equipped with a xenon excitation source (Horiba-Jobin Yvone Scientific Edison, NJ). Filtered surface- and floodplain-water extracts were normalized to 5 mg-C $L^{-1,}$ reducing inner-filter effects. Excitation emission matrices (EEMs) fluorescence scans were completed from 240 nm-600 nm excitation and emission wavelengths, with 3nm band-pass, 3nm increments, and 3 second integrations. A sealed cuvette of DI (>18

mΩ) was analyzed between every 10 samples to account for instrument drift and to minimize the influence of water Raman peaks in sample spectra. Scans were blank corrected using deionized water and corrected for inner filter effects (Kubista et al. 1994). First and second order Raleigh scattering were masked (10 nm width masking), and samples were normalized by the area of the deionized water Raman scattering peak (Lawaetz and Stedmon, 2009).

We used the fluorescence regional integration (FRI) approach to quantify five spectral regions (Matlab R2016b) as outlined by Chen et al. (2003). EEMS regions I and II are related to simple proteins (with similar fluorescence characteristics as tyrosine and tryptophan). Region III is related to lower molecular weight, aromatic compounds similar to fulvic acids. Region IV resembles soluble microbial byproducts, and region V is linked with polyaromatic compounds similar to lignin derivatives, tannins, and polyphenols (Chen et al., 2003; Fellman et al., 2010). As the FRI approach quantifies regions of wavelength-dependent fluorescent intensities, it is well suited to capture the underlying heterogeneity and compositional quality of dissolved organic matter leached from floodplain soils (Chen et al., 2003; Lynch, et al., 2019). Ultraviolet absorbance at the 254nm wavelength was divided by dissolved organic carbon concentration to calculate SUVA254 (L mg-C-1 m-1), an indicator of FDOM aromaticity or complexity (Weishaar et al., 2003).

Statistical Analysis

Statistical analyses were conducted in R statistical software (R Core Team, 2017). Differences in organic carbon (OC) storage per area within the three separate reservoirs and the sum of all three reservoirs between valley types was tested using Tukey HSD pairwise comparisons. For these comparisons, storage in wood, soil OC, and the sum of all three

reservoirs required log transformation to meet assumptions of normality and homoscedasticity, while OC storage in litter and duff required no transformation. Redundancy of variables in regression analyses was reduced by eliminating independent variables that were strongly cross-correlated with other variables or inherently linked to other variables by definition (Supplemental Tables S4, S5). For example, valley width was not considered when valley confinement was included as a variable, and width was not considered when examining potential predictors of floodplain sediment depth, which was normalized by valley width. Potential predictors for multiple linear regression to examine the depth of floodplain sediment and OC storage per area were selected using the following systematic process. The predictor most strongly correlated with the outcome variable was selected as the first predictor and all other variables highly correlated (r >7) with any previously selected variables were eliminated as possible predictors. Once variable selection was complete, exhaustive (backward and forward) stepwise multiple linear regression was conducted to determine the model that best explains the outcome variable as indicated by maximizing the Akaike Information Criterion (AIC; Akaike, 1998). Organic carbon storage per area was transformed using a boxcox power transformation (λ = -0.3838384) to meet the assumptions of normality and homoscedasticity for multiple linear regression to predict carbon storage among all three reservoirs (i.e., sediment, wood, and organic layer). No transformations were needed to meet these assumptions when predicting sediment depth normalized by valley width. We confirmed normality of model residuals by examining qq-plots, histograms, and failing to reject the null hypothesis of normality with an alpha level of 0.05 using the Shapiro-Wilk normality test, *shapiro.test* in R. Homoscedasticity was verified by failing to reject the null hypothesis with an alpha level of 0.05 for the studentized Breusch-Pegan test, *bptest* function in R. Principle components analysis was conducted on EEMS indices to

examine differences in the chemical composition of carbon in surface waters and floodplain leachates collected along intensive single thread-multithread-single thread reaches.

RESULTS

Carbon storage

Unconfined stream valleys store more OC (as the sum of litter, duff, large wood, and sediment) per area than more confined valleys in the study area, which is dominated by floodplain fine sediment. Within unconfined valleys, multithread reaches store less C than their single-thread counterparts (Figure 2; Table 2). Organic carbon storage in all valley types is dominated by the sediment and soil component. While comparable to litter and duff, large floodplain wood loads are the smallest reservoir for OC storage examined among the study reaches in the study area. Beaver meadows contain the lowest OC storage as large floodplain wood and as litter and duff among all channel types, whereas multithread channels store the most in these reservoirs. These differences reflect the abundance of old growth conifers in multithread reaches and the limited number of trees in beaver meadows, which store a substantial amount of OC in sediment and soil that is second only to unconfined single-thread channels. Unconfined single-thread reaches store significantly more OC in sediment compared to confined and partly confined channels, and significantly more organic carbon storage across all three reservoirs combined than confined channel reaches (Figure 2).

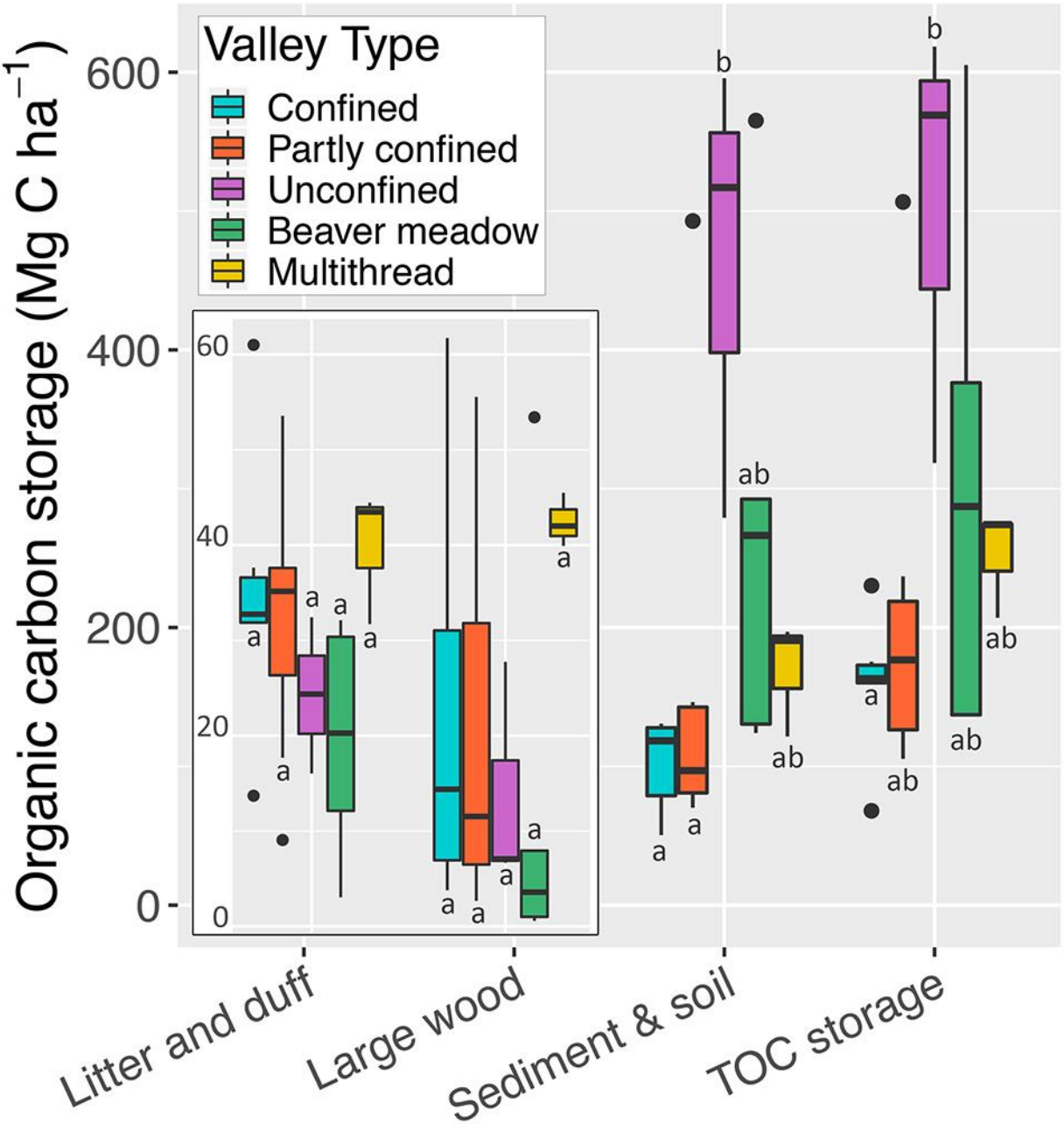

Figure 2. Bar plots of carbon storage per area representing the 24 study reaches in different valley types that vary by degree of confinement and channel complexity. TOC (total organic carbon) is the sum of organic carbon stored in litter and duff, large wood, and floodplain sediment and soil. Letters a and b indicate group assignments for channel types within each OC reservoir based on statistical significance at the 95% confidence level using Tukey HSD pairwise comparisons. Channel types sharing any combination of a or b are not significantly different, whereas channel types that do not share a common letter are significantly different.

Table 2. Floodplain organic carbon storage in litter + duff, large wood, and soil + fine sediment among all study reaches. Reaches are located along North St. Vrain Creek (NSV) and tributaries, Cony, Ouzel, and Hunters Creeks; the Big Thompson River (BTR) and tributary Mills Creek; Glacier Creek; and the South Fork Cache La Poudre River (SFP).

					Wood		Litter and humus		Soil and sediment				Total
Study Reach	**Stream**	**Valley type**	**Volume of sediment (m^3)**	**Valley area (ha)**	**Volume (m^3)**	**Carbon (MgC ha^{-1})**	**Volume (m^3)**	**Carbon (MgC ha^{-1})**	**Mean SOC (%)**	**Mean depth (cm)**	**Volume (m^3)**	**Carbon (MgC ha^{-1})**	**Carbon (MgC ha^{-1})**
CF1	NSV	Confined	229.8	0.09	16.8	36.5	82.4	61.0	3.0	25	229.8	67.7	165.3
CF2	Ouzel	Confined	47.3	0.02	6.6	61.7	19.3	37.6	6.6	22	47.3	130.8	230.1
CF3	Glacier	Confined	7.9	0.01	0.6	14.1	7.3	33.5	14.4	9	7.9	112.3	159.8
CF4	NSV	Confined	41.4	0.03	2.1	14.7	26.1	31.8	9.7	15	41.4	128.8	175.3
CF5	NSV	Confined	90.3	0.04	0.8	3.8	18.0	13.7	2.6	21	90.3	50.5	68.0
CF7	Glacier	Confined	59.4	0.04	0.9	4.6	27.6	32.0	8.7	16	59.4	124.5	161.1
PC1	NSV	Partly confined	590.0	0.30	17.5	11.5	209.9	37.7	4.4	19	590.0	76.7	126.0
PC2	Ouzel	Partly confined	100.6	0.06	15.8	55.5	47.4	35.0	9.2	18	100.6	146.3	236.8
PC3	Glacier	Partly confined	509.2	0.26	28.2	21.4	200.3	35.1	4.0	19	509.2	70.2	126.7
PC4	Hunters	Partly confined	169.1	0.05	10.7	42.2	40.0	37.5	3.2	33	169.1	96.9	176.7
PC5	NSVNSV	Partly confined	815.6	0.26	3.5	2.7	51.8	17.7	3.0	32	815.6	85.0	105.4
PC6	Glacier	Partly confined	193.0	0.05	1.1	4.7	14.4	9.1	13.2	42	193.0	492.8	506.6
PC7	NSV	Partly confined	1966.3	0.43	17.7	8.3	299.6	53.6	3.4	46	1966.3	139.0	200.8
UC1	Cony	Unconfined	402.4	0.13	18.4	27.8	47.1	24.4	19.0	30	402.4	516.9	569.1
UC2	Glacier	Unconfined	729.5	0.15	5.0	6.7	80.1	16.0	13.5	49	729.5	595.7	618.5
UC3	Mills	Unconfined	1186.3	0.21	7.4	7.1	173.6	32.4	5.4	57	1186.3	279.1	318.6
AB1	NSV	Beaver	3126.2	0.58	23.0	7.9	546.1	32.1	11.6	54	3126.2	565.1	605.2
AB2	Ouzel	Beaver	773.7	0.30	79.5	53.4	265.5	30.4	12.5	26	773.7	292.5	376.3
AB4	NSV	Beaver	28798.5	5.04	14.7	0.6	2109.6	20.3	5.2	57	28798.5	266.3	287.2
AB5	BTR	Beaver	19501.1	3.27	16.4	1.0	1090.6	12.1	2.3	60	19501.1	124.0	137.2
AB6	SFP	Beaver	4187.5	0.81	14.6	3.6	91.5	3.1	2.8	51	4187.5	130.4	137.1
MT1	NSV	Multithread	1269.3	0.49	103.1	42.0	558.5	43.5	5.2	26	1269.3	121.5	207.0
MT2	Glacier	Multithread	268.6	0.12	26.8	45.5	106.0	31.7	9.6	23	268.6	196.9	274.1
MT3	Ouzel	Multithread	881.7	0.37	74.1	39.9	452.4	44.5	8.9	24	881.7	190.7	275.1

The optimal stepwise multiple linear regression model (adjusted r^2=0.71, p<0.0001) explaining potential controls on the amount of OC storage per area (OC) includes elevation (z; p<0.001), stream gradient (S; p=0.01), and valley confinement (C_v; p=0.15).

$$OC = 0.349 - 8.17E\text{-}5z + 3.34E\text{-}1S - 1.11E\text{-}3C_v \quad (1)$$

Elevation and stream gradient are significant predictors variables at the 99% confidence level. Results indicate that organic carbon storage per area – where a negative power transformation inverted the sign of the regression coefficients relative to the correlation (Table S4) – is highest at higher elevation, low-gradient streams, that are less confined.

Higher OC storage per area along unconfined single-thread channels is linked to deeper sediment and higher OC content along those valley types. Beaver meadows and unconfined single-thread channels have significantly higher mean floodplain sediment depth, which is significant when compared to confined channel reaches ($p < 0.01$; Figure 3A). Unconfined single-thread study reaches also have the highest mean OC content across all channel types – although these differences are not significantly higher in unconfined study reaches – and substantially more than multithread channel reaches (Figure 3B),

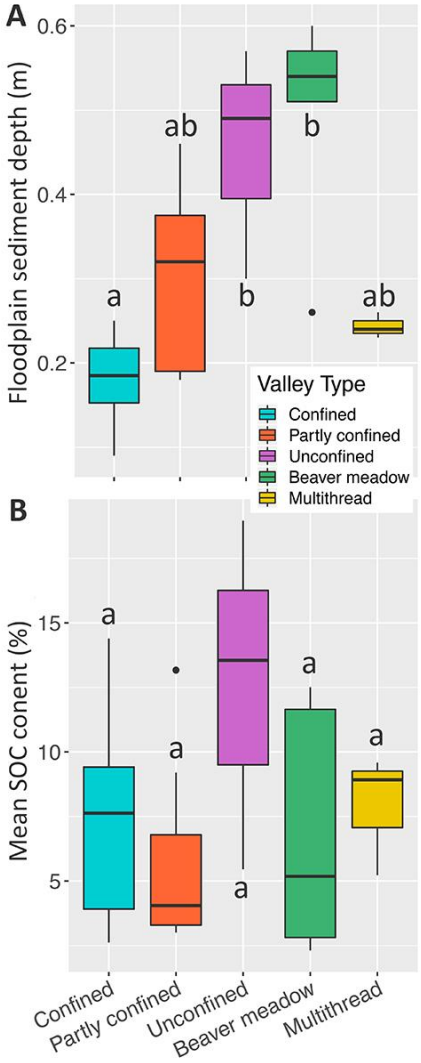

Figure 3. Boxplots of floodplain soil depth and mean soil organic carbon content (SOC) by valley type. Letters a and b indicate group assignments for channel types within each OC reservoir based on statistical significance at the 95% confidence level using Tukey HSD pairwise comparisons. Channel types sharing any combination of a or b are not significantly different, whereas channel types that do not share a common letter are significantly different.

Logjams and fine sediment storage

The optimal model from stepwise multiple linear regression indicates that ~74% of the variability in average floodplain sediment depths (p=0.047), standardized by valley width (d_w), is best explained by the six-year average number of logjams (λ; p = 0.04), stream gradient (S; p = 0.04), drainage area (A; p = 0.16), and elevation (z; p = 0.30).

$$d_w = -9.11\,E^{-2} - 6.77\,E^{-4}\,A + 3.53\,E^{-5}\,z + 1.6\,E^{-1}\,S - 2.4\,E^{-3}\,\lambda \quad (2)$$

This means that the frequency of logjams within a given river segment is linked with decreased depth of floodplain fine sediment accumulation when considering valley width and stream gradient (Supplemental Table S5).

Organic matter composition along intensive study segments

Using principal components analysis, we identified relationships between channel complexity and the characteristics of fluorescing dissolved organic matter (FDOM) collected from stream flow and adjacent floodplain soils in the single thread-multithread-single thread intensive study segments (Figure 4). Stream water flowing from confined reaches into multithread channel reaches had optical properties consistent with terrestrially derived organic acids (regions III and V; Figure 4A). FDOM complexity ($SUVA_{254}$) and the relative abundance of protein-like compounds (EEMS regions I, II) that are typically associated with microbial sources (Lynch, et al., 2019) increased within multithread networks. Regions II and V were also more variable within multithread reaches, which may reflect more diverse pathways for microbial transformation of terrestrially-derived C. Surface water flowing through lower confined reaches retained the signature imparted by multithread channels, with relatively more proteinaceous features than upper confined reaches.

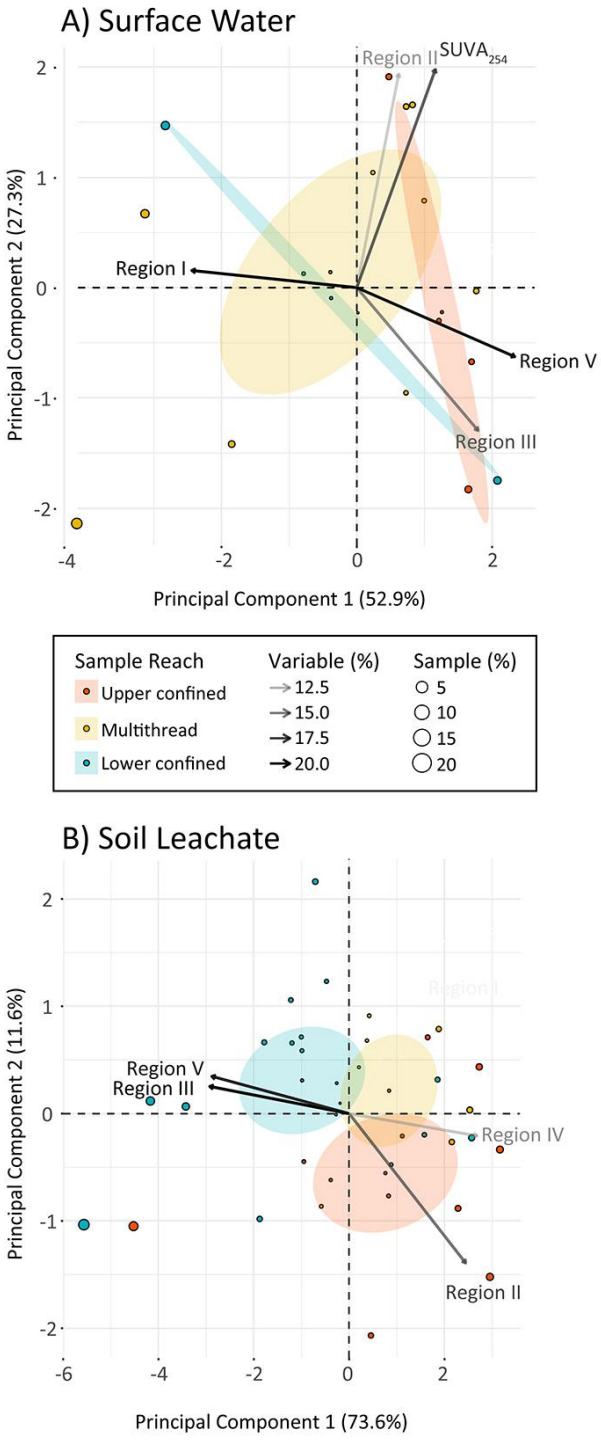

475

476 **Figure 4.** Principal components analysis (PCA) of UV-Fluorescence properties as a function of
477 channel complexity and source. The contribution (in percent) of individual variables (vector
478 shade) and samples (symbol size) to principal components 1 and 2 are shown. Shaded ellipses
479 correspond to 95% confidence intervals for the upper, lower, and multithread reaches. Data input
480 to PCA analysis provided in Supplemental Table S6 and additional data available as stated in the
481 acknowledgements.

EEMS spectra of floodplain soil leachate contained a similar, but opposite, shift in the signatures of organic matter at the study sites. The relative intensities of EEMS regions II and IV (representing simple proteins and byproducts of microbial metabolism) were highest in soil leachate collected from upper, confined reaches flowing into multithread channels (Figure 4B). Similar to the pattern found in surface waters, the fluorescent properties of floodplain soil leachates within multithread reaches reflected both terrestrial and microbial-derived OC. However, the variability in fluorescence spectra of floodplain leachates collected from multithread reaches was more constrained, relative to upstream and downstream single-thread reaches, than that found in adjacent surface waters (Figure 4B). Floodplain soil leachates collected from lower, confined reaches had higher relative percent intensities of regions III and V, reflecting a more diverse array of terrestrially-derived organic acids relative to the upstream reach. In both surface waters and floodplain soil leachates, DOM variability was highest in multithread reaches. Although DOM variability simplifies as multithread channels converge into a single-thread planform, the complexity of DOM within multithread reaches is somewhat retained within lower single-thread reaches compared to upper confined channels. These transformations have important implications for substrate quality as DOM is exported to higher-order river networks.

Discussion

Multithread channel carbon storage

The data presented here confirms prior research that unconfined valleys store more carbon per area than confined valleys (Wohl et al., 2012), but in contrast to this past work unconfined single-thread channels and beaver meadows store relatively more OC per area than

their complex logjam-induced multithread channel counterparts. While OC storage in beaver meadows was not as high as unconfined single-thread channel reaches, they do constitute substantial storage. Additional research in the study area yields similar values to those we present here for OC storage in beaver meadows, but suggests OC storage decreases when meadows are abandoned by beavers (Wohl, 2013; Laurel & Wohl, 2019). Decreases in OC storage following decline in local water tables and long-term decreases in hydrologic connectivity may reflect decreased fluvial deposition of OM across the floodplain and decreased *in-situ* production of OM by riparian vegetation after streams incise following abandonment by beavers. Seasonal changes in hydrologic connectivity have also been correlated with shifts in the molecular composition of OM flowing through multithread beaver meadows (Lynch, et al. 2019), such that the breakdown of complex OM increased following losses in hydrologic connectivity during base-flow conditions. Our observations that OC content of sediment is higher in single-thread channel reaches and lower in multithread channel reaches suggest similar hydrologic controls regarding connectivity as a catalyst to OM transformation.

Lower OC storage in the floodplain sediments of multithread channels are driven by two primary characteristics among the study reaches: (1) limited sediment storage capacity and (2) lower OC content. Our results inform two conceptual models that explain the observed decreases in sediment depth and OC content along multithread reaches.

Floodplain sediment depth and storage

The mean depth of floodplain fine sediment along single-thread channels in unconfined valleys (45 ± 14 cm) is substantially deeper (although not significantly $p = 0.28$) than that along multithread channel reaches (24 ± 2 cm; Figure 3.). This corresponds to decreased sediment

528 volume per valley width and associated OC that can be stored per area in multithread reaches
529 versus unconfined single-thread reaches with similar valley widths. Recruitment of old-growth
530 trees into the stream channel and the formation of channel-spanning logjams has been shown to
531 facilitate floodplain aggradation and complex topography in headwater streams (Sear et al.,
532 2010), resulting in the stabilization of vegetated islands and storage of fine sediment in large
533 alluvial valleys (Collins et al., 2012). In work conducted here along smaller streams (<200 km^2),
534 multiple channels of flow across the valley bottoms appear to limit total sediment storage for
535 valleys of similar width.
536 Because flow is dispersed across numerous channels in these multithread systems, energy
537 to mobilize gravel is reduced, but sand and silt are still easily transported in smaller side
538 channels with shallower flow (Figure 5). The boundary shear stress (τ_b) acting on the channel
539 bed is defined as
540 $$\tau_b = \rho_w g h S \qquad \text{(equation 3)}$$
541 where ρ_w is the density of water, g is the force of gravity, S is the frictional channel slope,
542 and h represents the depth of flow. Estimated dimensionless bed shear stress (τ_b^*) used to
543 determine initial motion of particles of a median grain size on the bed is calculated as
544 $$\tau_b^* = \frac{\tau_b}{(\rho_s - \rho_w) g D} \qquad \text{(equation 4)}$$
545 where D is median grain size, and ρ_s is the mean density of the sediment grain. Because
546 incipient motion of sediment in the channel and on the floodplain is dependent upon critical
547 shear stress (τ_c*) values for an individual or median grain size, sediment transport occurs when
548 $$\tau_b^* > \tau_c^* \qquad \text{(equation 5)}$$
549 Assuming a constant dimensionless critical shear stress (τ_c*) value of 0.03, derived from the
550 Shields diagram for the initial motion of grains in a nonuniform gravel-bed river (Parker, 1990),

551 the threshold necessary to mobilize the median grain size in the study area (~12 cm; Livers &
552 Wohl, 2015) is easily met during high flows in a single-thread channel (Figure 5A). This
553 threshold is less likely to be met when discharge is distributed across several channels (Figure
554 5B).

555 At high flows, shear stress is partitioned across multiple channels and large in-stream
556 wood, which dissipates a disproportionate amount of that increased shear stress (Manga &
557 Kirchner, 2000). Because critical shear stress for coarser fractions increases with increasing
558 slope (Lamb et al., 2008), steeper slopes of the multithread channel reaches in our study (Table
559 1) may compound the partitioning of shear stress across the valley floor, requiring higher flow
560 depths to transport gravel and cobbles along multithread reaches. Continuous transport of finer
561 sediment, limited competence to mobilize coarser sediment, the accumulation of gravels behind
562 logjams (Cadol & Wohl, 2011), and divergence of flow around logjams could work in tandem to
563 facilitate bank erosion, undercutting of trees, and channel avulsions (Sear et al., 2010; Polvi &
564 Wohl, 2013).

565 In contrast with the characteristics of multithread channels described above, single-thread
566 unconfined channel floodplains dominated by densely growing rushes, sedges, and woody shrubs
567 stabilize channel banks and provide resistance to erosion (Simon & Collison, 2002; Figure 5C).
568 Dissipation of energy across the broad floodplains of single-thread channels results in the
569 accumulation of fine overbank sediment. Fine sediment provides additional cohesion and
570 resistance to erosion, floodplain aggradation, the ability of the channel to convey larger flows,
571 and the accumulation of *in situ* organic matter from floodplain vegetation. Together, these
572 processes can significantly increase OC storage per area.

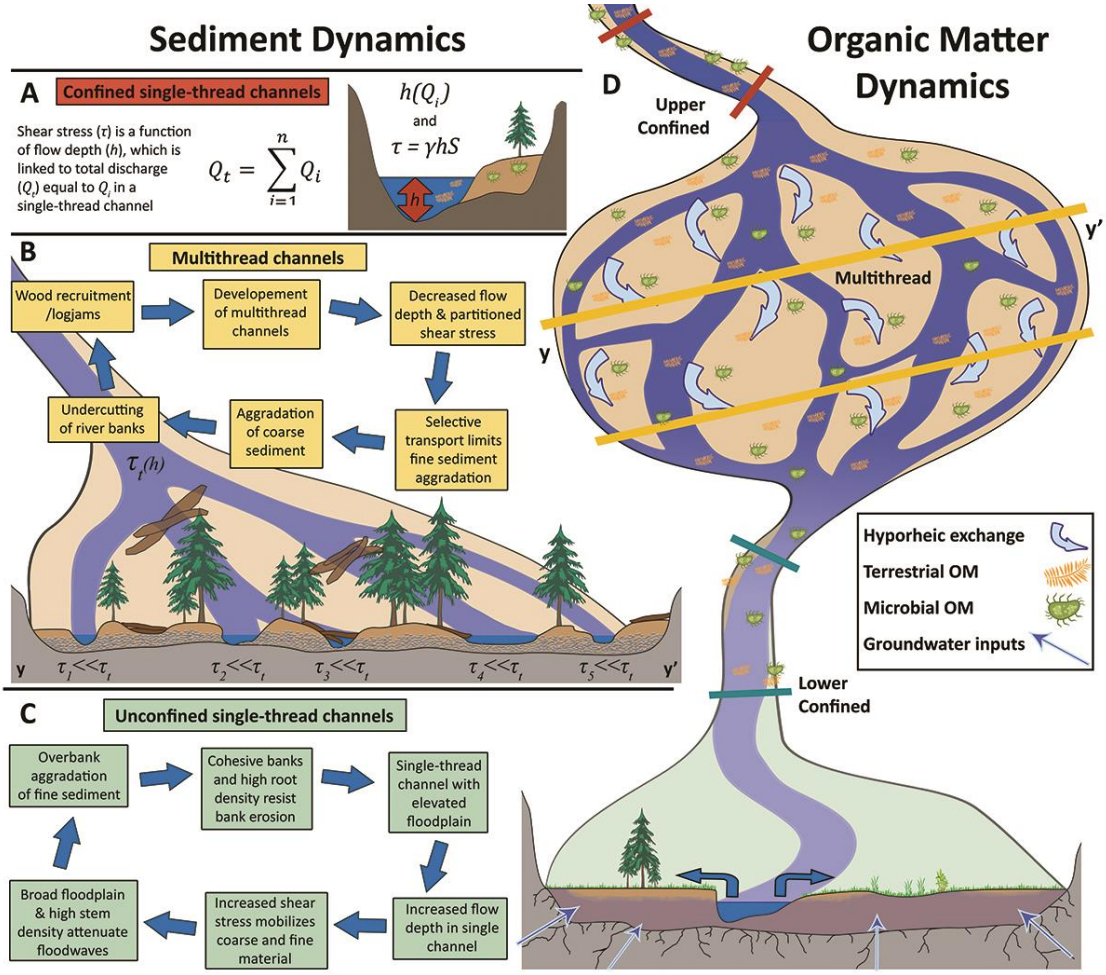

Figure 5. Conceptual figure of sediment dynamics in (A) confined, (B) multithread, and (C) unconfined systems and observed dissolved organic matter dynamics in (D) single thread-multithread-single thread transitional stream segments. (A) Shear stress (τ) is a function of the specific weight of water (γ), stream gradient (S), and flow depth (h), which changes with discharge (Q). In multithread channels (B) where $Q_t = Q_1 + Q_2 + Q_3 + ... Q_n$ for n number of channels, flow depth is not additive as is Q_t so h, and thus τ, decrease substantially across the valley bottom. Increased transit time and hyporheic exchange in multithread channels facilitates extraction and mixing of terrestrial and microbial organic matter (OM) from floodplain sediment, increasing the transformation and mineralization of OM and resulting in higher OM diversity within multithread and downstream (D) systems. Unconfined single-thread channels have high *in situ* OM inputs from seasonal sedges and evidence of groundwater inputs that may cause higher observed OC concentrations (C).

Floodplain organic carbon content and diversity

Multithread reaches contain lower OC content in floodplain fine sediments than their single-thread counterparts flowing through relatively unconfined valleys (Table 2). This result is

590 linked to two primary observations: (1) differences in OC sources and (2) inferred differences in
591 the transit time of water and entrained OC in the two valley types.
592 Although we assume that a substantial portion of OC inputs to floodplains in the study
593 area are fluvially transported, relative proportions of *in-situ* sources of OC likely differ between
594 logjam-induced multithread reaches and unconfined valley segments. The dominant source of *in-*
595 *situ* floodplain OC at our multithread study reaches, which lack abundant vegetative ground
596 cover, is likely coarse particulate organic matter sourced from and retained by large wood
597 (Quinn et al., 2007; Beckman & Wohl, 2014). In contrast, sources of floodplain OC along
598 unconfined single-thread reaches appear to be dominated by continuous *in-situ* production of
599 perennial rushes and sedges and their dense root mats. Two of three unconfined single-thread
600 channels in this study contain higher OC content (>13%) than multithread reaches (all <10%),
601 which may reflect continuous annual production of OM from perennial vegetation. Higher OC
602 content could also reflect saturation of floodplain soils, which we observed even at low flow
603 conditions late in the year, along the two single-thread channels in unconfined valleys.
604 Higher moisture content within unconfined single-thread floodplains could facilitate
605 positive feedbacks between moisture content and bedrock weathering or moisture content and
606 tree growth. Increased moisture at the bedrock/regolith interface could increase chemical
607 weathering and bedrock fracturing, which in turn could increase groundwater input into these
608 reaches (Figure 5D). Although it is possible that groundwater could contain OC and increase OC
609 levels along floodplains experiencing groundwater discharge, organic-rich sedimentary rocks are
610 virtually non-existent in the study area (Braddock & Cole, 1990). Abundant moisture along these
611 floodplains within old growth forests, however, may also limit (1) conifer growth, (2) wood
612 recruitment to channels, (3) logjams, and (4) the transition into multithread channel systems,

613 creating a stable state for moist grassy floodplains without abundant conifers. These conditions
614 contrast substantially with multithread channels, which are not dominated by grasses, does not
615 contain the same evidence for groundwater inputs, and instead likely experience abundant
616 hyporheic flow.

617 Higher relative abundance of soluble proteins and microbial byproducts in the surface
618 waters and adjacent floodplain leachates of complex multithread stream reaches – relative to
619 more confined, single-thread channels – suggests complex channels are biogeochemical hotspots
620 for the transformation of DOM. The longer residence time within these complex reaches allows
621 terrestrial-derived organic matter (e.g. lignin-derivatives and higher molecular weight organic
622 acids) to be compositionally altered via microbial transformation or photo-oxidation. The
623 assimilation and transformation of OC within complex, bio-reactive stream reaches may reduce
624 OC concentrations as a result of retention within microbial biomass and CO_2 mineralization.

625 Downstream shifts in DOM composition within the Glacier and Ouzel Creek intensive
626 study segments provide mechanistic insight into hyporheic exchange and mixing that occurs
627 between in-stream and floodplain sediment (Figure 5D). Surface water DOM chemistry in
628 single-thread channels upstream of multithread systems is characteristic of organic matter
629 sourced from terrestrial inputs. In contrast, floodplain sediments in these single-thread reaches
630 reflected the signatures of microbial activity working to break down that OM (Figure 5D).
631 Complex channel planform, heterogeneity of channel bedforms, and channel boundary
632 irregularities in multithread reaches promote: increased hyporheic exchange, longer transit times
633 for water and entrained DOM, greater oxygen availability, diversity in microbial community
634 structure (Danczak et al., 2016; Gooseff et al., 2007), oxidation of organic matter (Battin et al.,
635 2008; Boye et al., 2017), flushing of OM from floodplain sediment, and mixing of organic matter

pools in both sediment and surface waters (Stegen et al., 2016; Figure 5D). As a result, microbial and invertebrate communities have greater opportunities to assimilate and transform organic matter, reducing OC storage through CO_2 mineralization to the atmosphere. Greater heterogeneity of the fluorescing DOM pool, as well as a higher relative abundance of protein-rich microbial derivatives in multithread channels is reflected in the downstream composition of DOM in surface waters and sediment. Allochthonous signatures likely reflect fluvial transport of complex terrestrial DOM from upstream multithread reaches, where wood, litter, duff, and hyporheic exchange is abundant.

Hotspots for ecosystem productivity

Findings presented here support past work that identifies morphologically complex multithread streams as hotspots for the decomposition and transformation of OC (Battin et al., 2008; Lynch, et al., 2019). These complex channels in the Colorado Front Range facilitate food webs that support observed increases in aquatic invertebrate, rainbow trout, and cutthroat trout biomass relative to less-complex, single-thread channels (Livers & Wohl, 2016; Wohl, Lininger, et al., 2017; Herdrich et al., 2018; Venarsky et al., 2018). Here we show that the potential increase in microbial activity and decomposition of organic matter along complex multithread reaches may provide the resources necessary at the bottom of the food web to facilitate increased productivity in these mountainous streams systems.

Terrestrial carbon dynamics, climate change, and land use

Incorporating floodplain C dynamics into the terrestrial OC budget requires investigating potential changes in floodplain dynamics that could shift sediment and OC floodplain reservoirs

658 out of equilibrium. Otherwise, rivers are simply neutral pipes (Cole et al., 2007), with no change
659 in storage or significant influence on terrestrial C budgets on annual or decadal time scales.
660 The dynamic nature of rivers and their sensitivity to anticipated changes in precipitation
661 and hydrologic flow regimes are poised to trigger changes in sediment dynamics and hydrologic
662 connectivity that may shift the role of floodplains as OC sinks or sources to inland and coastal
663 waters (N. A. Sutfin et al., 2016). Observed decreases in snowpack and earlier snowmelt
664 (Stewart, 2009), elevational shifts in rain-snow transitions (Kampf & Lefsky, 2016), changes in
665 precipitation regimes – including potential for extreme precipitation and rain-on-snow events –
666 may drastically alter flow regimes (Bates et al., 2008) and carbon dynamics in fluvial corridors
667 (N. A. Sutfin et al., 2016). Extreme floods associated with projected changes in flow regimes
668 (Bates et al., 2008) and increases in the frequency and severity of wildfire (Westerling et al.,
669 2006; Abatzoglou & Williams, 2016) have the potential to greatly alter floodplain sediment
670 residence times (N. A. Sutfin & Wohl, 2019) and C storage along river corridors (Wohl et al.,
671 2020). In addition, predicted changes in hydrology associated with climate change (Bates et al.,
672 2008), including potential for extreme drought (Trenberth et al., 2014), are projected to alter
673 hydrologic lateral and longitudinal connectivity with impacts to local ground water tables, rates
674 of hyporheic exchange, and soil moisture (Alexander et al., 2015), which collectively regulate
675 the potential for OC storage and decomposition (N. A. Sutfin et al., 2016).
676 Shifts in carbon storage and transformation are likely to respond in diverse ways as a
677 result of channel form and associated processes presented here. Decreases lateral connectivity
678 across valley bottoms with single-thread channels, for example, is likely to decrease overbank
679 aggradation of fine sediment, germination and growth of riparian vegetation, and resulting OC
680 storage. These same changes in hydrologic regime in multithread channels could decrease

hyporheic exchange, moisture content, wetting and drying cycles, and available oxygen important for the microbial transformation of OC that we present here.

Land use, flow regulation, channel manipulation, deforestation, and reduced channel complexity that accompany growing populations and increased demand for freshwater exacerbate changes in hydrologic flow regime and available moisture, which can greatly alter OC dynamics and the potential for OC storage along river corridors (Wohl, et al., 2017). Reservoir impoundments, diversions, and resulting decreases in peak flow magnitude and lateral connectivity are likely to decrease floodplain OC accumulation and storage. Urbanization, channelization, increased impervious surfaces, deforestation, in-stream wood removal, flow augmentations, and flow regulation that increases baseflow conditions are likely to produce artificially elevated discharge and effects similar to climate-induces flooding mentioned above. However, new accommodation space for OC uptake as a result of human-induced erosion (Berhe et al., 2007; Oost et al., 2012; T. Hoffmann et al., 2013; Wang et al., 2017), extreme floods or slope failures, and pyrogenic sequestration by wildfire (Santín et al., 2015; Jones et al., 2019) may have substantial influence on offsetting global C emissions through burial of organic matter.

CONCLUSION

Mountainous headwater streams are important components of the terrestrial carbon cycle, including long-term storage and ecosystem productivity. Results presented here indicate that organic carbon storage along river corridors of the Colorado Front Range is highest in relatively unconfined, low-gradient valleys at high elevations. Aggradation of floodplain fine sediment and storage of OC appears limited where single-thread channels in unconfined valleys are forced into multithread channel planforms by persistent channel-spanning logjams. Conversely, flood-wave

attenuation across unconfined valleys dissipates energy and allows the deposition of fine sediment along elevated, cohesive floodplains of single thread channels with abundant grasses. We posit that decreased flow depth and shear stress available to transport coarser sediment as a result of higher flows spreading across numerous channels in multithread streams limit the aggradation of fine sediment and OC storage per area. In addition to reduced storage of fine sediment in multithread reaches, these complex systems act as hotspots for the transformation and mineralization of OM, resulting in decreased OC storage. Increased microbial activity and decomposition of OM, which are food sources for aquatic invertebrates, support observations by others that link channel complexity with increased biomass productivity in fish. Observed and predicted changes in snowpack, snowmelt, flow regimes, and extreme events exacerbated by water demand and land use are likely to greatly influence the hydrologic connectivity and channel complexity associated with sediment and carbon dynamics presented here.

ACKNOWLEDGEMENTS AND DATA

This paper is based upon work supported by National Science Foundation Grant No. DGE-0966346 "I-WATER: Integrated Water, Atmosphere, Ecosystems Education and Research Program" at Colorado State University (CSU); NSF Doctoral Research Dissertation Improvement Grant #1536186; and graduate student research grants from the Geological Society of America, the Colorado Scientific Society, and the Colorado State University Warner College of Natural Resources and Department of Geosciences. We thank Rocky Mountain National Park their support with a research permit, Teagan Deeney and Jim Self at the CSU Soil and Water Laboratory, Mark Pascke for use of his lab, Thomas Borch for his insight and guidance, and assistance in the field and the laboratory by Ben Von Thaden, Dean Anderson, John Harris,

Matheus Cruz Lima Pereira, Bryce Johnson, Julia Makiejus, Pamela Wagener, Jon Garber, Joel Sholtes, and Fernando Javier Ugalde Pascual. All data generated in this study can be accessed through the associated Supplemental Information file, http://hdl.handle.net/10217/173334, and Sutfin (2020) cited below.

References

Abatzoglou, J. T., & Williams, A. P. (2016). Impact of anthropogenic climate change on wildfire across western US forests. *Proceedings of the National Academy of Sciences*, *113*(42), 11770–11775. https://doi.org/10.1073/pnas.1607171113

Akaike, H. (1998). A New Look at the Statistical Model Identification. In E. Parzen, K. Tanabe, & G. Kitagawa (Eds.), *Selected Papers of Hirotugu Akaike* (pp. 215–222). New York, NY: Springer New York. https://doi.org/10.1007/978-1-4612-1694-0_16

Alexander, L., Autrey, B., DeMeester, J., & Fritz, K. M. (2015). *Connectivity of Streams and Wetlands to Downstream Waters: A Review and Synthesis of the Scientific Evidence* (Reports & Assessments No. EPA/600/R-14/475F) (p. 408). The U.S. Environmental Protection Agency's (USEPA) Office of Research and Development.

Anderson, R. S., Riihimaki, C. A., Safran, E. B., & MacGregor, K. R. (2006). Facing reality: Late Cenozoic evolution of smooth peaks, glacially ornamented valleys, and deep river gorges of Colorado's Front Range. *SPECIAL PAPERS-GEOLOGICAL SOCIETY OF AMERICA*, *398*(397).

Aufdenkampe, A. K., Mayorga, E., Raymond, P. A., Melack, J. M., Doney, S. C., Alin, S. R., et al. (2011). Riverine coupling of biogeochemical cycles between land, oceans, and atmosphere. *Frontiers in Ecology and the Environment*, *9*(1), 53–60. https://doi.org/10.1890/100014

Ballantyne, A. P., Alden, C. B., Miller, J. B., Tans, P. P., & White, J. W. C. (2012). Increase in observed net carbon dioxide uptake by land and oceans during the past 50 years. *Nature*, *488*(7409), 70–72. https://doi.org/10.1038/nature11299

Barry, R. G. (1973). A Climatological Transect on the East Slope of the Front Range, Colorado. *Arctic and Alpine Research*, *5*(2), 89–110. https://doi.org/10.1080/00040851.1973.12003684

Bates, B., Kundzewicz, Z. W., Wu, S., & Palutikof, J. (2008). *Climate Change and Water. Technical Paper of the Intergovernmental Panel on Climate Change* (Technical Paper VI No. VI) (p. 210). Geneva: IPCC Secretariat. Retrieved from https://digital.library.unt.edu/ark:/67531/metadc11958/m1/13/

Battin, T. J., Kaplan, L. A., Findlay, S., Hopkinson, C. S., Marti, E., Packman, A. I., et al. (2008). Biophysical controls on organic carbon fluxes in fluvial networks. *Nature Geoscience*, *1*(2), 95–100. https://doi.org/10.1038/ngeo101

Battin, T. J., Luyssaert, S., Kaplan, L. A., Aufdenkampe, A. K., Richter, A., & Tranvik, L. J. (2009). The boundless carbon cycle. *Nature Geoscience*, *2*(9), 598–600. https://doi.org/10.1038/ngeo618

Beckman, N. D., & Wohl, E. (2014). Carbon storage in mountainous headwater streams: The role of old-growth forest and logjams. *Water Resources Research*, *50*(3), 2376–2393. https://doi.org/10.1002/2013WR014167

Berhe, A. A., Harte, J., Harden, J. W., & Torn, M. S. (2007). The Significance of the Erosion-induced Terrestrial Carbon Sink. *BioScience*, *57*(4), 337–346. https://doi.org/10.1641/B570408

Birkeland, P. W., Shroba, R. R., Burns, S. F., Price, A. B., & Tonkin, P. J. (2003). Integrating soils and geomorphology in mountains—an example from the Front Range of Colorado. *Geomorphology*, *55*(1), 329–344. https://doi.org/10.1016/S0169-555X(03)00148-X

771 Borch, T., Kretzschmar, R., Kappler, A., Cappellen, P. V., Ginder-Vogel, M., Voegelin, A., & Campbell, K.
772 (2010). Biogeochemical Redox Processes and their Impact on Contaminant Dynamics.
773 *Environmental Science & Technology*, *44*(1), 15–23. https://doi.org/10.1021/es9026248
774 Boye, K., Noël, V., Tfaily, M. M., Bone, S. E., Williams, K. H., Bargar, J. R., & Fendorf, S. (2017).
775 Thermodynamically controlled preservation of organic carbon in floodplains. *Nature Geoscience*,
776 *10*(6), 415–419. https://doi.org/10.1038/ngeo2940
777 Braddock, W. A., & Cole, J. C. (1990). Geologic map of Rocky Mountain National Park and vicinity,
778 Colorado. U.S. Geological Survey.
779 Cadol, D., & Wohl, E. (2011). Coarse sediment movement in the vicinity of a logjam in a neotropical
780 gravel-bed stream. *Geomorphology*, *128*(3), 191–198.
781 https://doi.org/10.1016/j.geomorph.2011.01.007
782 Chapin, F. S., Matson, P. A., & Vitousek, P. (2011). *Principles of Terrestrial Ecosystem Ecology* (2nd ed.).
783 New York, NY: Springer Science & Business Media.
784 Chen, W., Westerhoff, P., Leenheer, J. A., & Booksh, K. (2003). Fluorescence excitation - emission matrix
785 regional integration to quantify spectra for dissolved organic matter. *Environmental Science and*
786 *Technology*, *37*(24), 5701–5710.
787 Cole, J. J., Prairie, Y. T., Caraco, N. F., McDowell, W. H., Tranvik, L. J., Striegl, R. G., et al. (2007). Plumbing
788 the Global Carbon Cycle: Integrating Inland Waters into the Terrestrial Carbon Budget.
789 *Ecosystems*, *10*(1), 172–185. https://doi.org/10.1007/s10021-006-9013-8
790 Collins, B. D., Montgomery, D. R., Fetherston, K. L., & Abbe, T. B. (2012). The floodplain large-wood cycle
791 hypothesis: A mechanism for the physical and biotic structuring of temperate forested alluvial
792 valleys in the North Pacific coastal ecoregion. *Geomorphology*, *139–140*, 460–470.
793 https://doi.org/10.1016/j.geomorph.2011.11.011

Danczak, R. E., Sawyer, A. H., Williams, K. H., Stegen, J. C., Hobson, C., & Wilkins, M. J. (2016). Seasonal hyporheic dynamics control coupled microbiology and geochemistry in Colorado River sediments. *Journal of Geophysical Research: Biogeosciences*, *121*(12), 2976–2987. https://doi.org/10.1002/2016JG003527

D'Elia, A. H., Liles, G. C., Viers, J. H., & Smart, D. R. (2017). Deep carbon storage potential of buried floodplain soils. *Scientific Reports*, *7*(1), 8181. https://doi.org/10.1038/s41598-017-06494-4

Downing, J. A., Cole, J. J., Duarte, C. M., Middelburg, J. J., Melack, J. M., Prairie, Y. T., et al. (2012). Global abundance and size distribution of streams and rivers. *Inland Waters*, *2*(4), 229–236. https://doi.org/10.5268/IW-2.4.502

Falkowski, P., Scholes, R. J., Boyle, E., Canadell, J., Canfield, D., Elser, J., et al. (2000). The Global Carbon Cycle: A Test of Our Knowledge of Earth as a System. *Science*, *290*(5490), 291–296. https://doi.org/10.1126/science.290.5490.291

Fellman, J. B., Hood, E., & Spencer, R. G. M. (2010). Fluorescence spectroscopy opens new windows into dissolved organic matter dynamics in freshwater ecosystems: A review. *Limnology and Oceanography*, *55*(6), 2452–2462. https://doi.org/10.4319/lo.2010.55.6.2452

Fetherston, K. L., Naiman, R. J., & Bilby, R. E. (1995). Large woody debris, physical process, and riparian forest development in montane river networks of the Pacific Northwest. *Geomorphology*, *13*(1), 133–144. https://doi.org/10.1016/0169-555X(95)00033-2

FIA. (2019). *Forest Inventory and Analysis National Program - FIA Library*. Washington, D.C.: U.S. Forest Service, FIA Program. Retrieved from https://www.fia.fs.fed.us/library/field-guides-methods-proc/

Galy, V., Peucker-Ehrenbrink, B., & Eglinton, T. (2015). Global carbon export from the terrestrial biosphere controlled by erosion. *Nature*, *521*(7551), 204–207. https://doi.org/10.1038/nature14400

Glass, S. V., & Zelinka, S. L. (2004). *Wood Handbook Ch 4: Moisture Relations and Physical Properties of Wood* (USDA General Technical Report No. FPL-GTR-190) (p. 20). Madison, WI: U.S. Department of Agriculture, Forest Service, Forest Products Laboratory. Retrieved from https://www.fpl.fs.fed.us/documnts/fplgtr/fplgtr190/chapter_04.pdf

Gooseff, M. N., Hall, R. O., & Tank, J. L. (2007). Relating transient storage to channel complexity in streams of varying land use in Jackson Hole, Wyoming. *Water Resources Research*, *43*(1). https://doi.org/10.1029/2005WR004626

Gregory, J. M., Jones, C. D., Cadule, P., & Friedlingstein, P. (2009). Quantifying Carbon Cycle Feedbacks. *Journal of Climate*, *22*(19), 5232–5250. https://doi.org/10.1175/2009JCLI2949.1

Gurnell, A. M., Petts, G. E., Hannah, D. M., Smith, B. P. G., Edwards, P. J., Kollmann, J., et al. (2000). Wood storage within the active zone of a large European gravel-bed river. *Geomorphology*, *34*(1), 55–72. https://doi.org/10.1016/S0169-555X(99)00131-2

Guyette, R. P., Cole, W. G., Dey, D. C., & Muzika, R.-M. (2002). Perspectives on the age and distribution of large wood in riparian carbon pools. *Canadian Journal of Fisheries and Aquatic Sciences*, *59*(3), 578–585. https://doi.org/10.1139/f02-026

Herdrich, A. T., Winkelman, D. L., Venarsky, M. P., Walters, D. M., & Wohl, E. (2018). The loss of large wood affects rocky mountain trout populations. *Ecology of Freshwater Fish*, *27*(4), 1023–1036. https://doi.org/10.1111/eff.12412

Hoffmann, T., Mudd, S. M., Oost, K. van, Verstraeten, G., Erkens, G., Lang, A., et al. (2013). Short Communication: Humans and the missing C-sink: erosion and burial of soil carbon through time. *Earth Surface Dynamics; Gottingen*, *1*(1), 45–52. http://dx.doi.org/10.5194/esurf-1-45-2013

Hoffmann, Thomas, Glatzel, S., & Dikau, R. (2009). A carbon storage perspective on alluvial sediment storage in the Rhine catchment. *Geomorphology*, *108*(1–2), 127–137. https://doi.org/10.1016/j.geomorph.2007.11.015

Huang, W., Peng, P., Yu, Z., & Fu, J. (2003). Effects of organic matter heterogeneity on sorption and desorption of organic contaminants by soils and sediments. *Applied Geochemistry*, *18*(7), 955–972. https://doi.org/10.1016/S0883-2927(02)00205-6

Hyatt, T. L., & Naiman, R. J. (2001). The Residence Time of Large Woody Debris in the Queets River, Washington, Usa. *Ecological Applications*, *11*(1), 191–202. https://doi.org/10.1890/1051-0761(2001)011[0191:TRTOLW]2.0.CO;2

Ives, R. L. (1942). The beaver-meadow complex. *Journal of Geomorphology*, *5*(3), 191–203.

Jarrett, R. D. (1990). Paleohydrologic techniques used to define the spatial occurrence of floods. *Geomorphology*, *3*(2), 181–195. https://doi.org/10.1016/0169-555X(90)90044-Q

Jones, M. W., Santín, C., Werf, G. R. van der, & Doerr, S. H. (2019). Global fire emissions buffered by the production of pyrogenic carbon. *Nature Geoscience*, *12*(9), 742–747. https://doi.org/10.1038/s41561-019-0403-x

Kampf, S. K., & Lefsky, M. A. (2016). Transition of dominant peak flow source from snowmelt to rainfall along the Colorado Front Range: Historical patterns, trends, and lessons from the 2013 Colorado Front Range floods. *Water Resources Research*, *52*(1), 407–422. https://doi.org/10.1002/2015WR017784

Lamb, M. P., Dietrich, W. E., & Venditti, J. G. (2008). Is the critical Shields stress for incipient sediment motion dependent on channel-bed slope? *Journal of Geophysical Research: Earth Surface*, *113*(F2). https://doi.org/10.1029/2007JF000831

Laurel, D., & Wohl, E. (2019). The persistence of beaver-induced geomorphic heterogeneity and organic carbon stock in river corridors: Beaver-induced heterogeneity. *Earth Surface Processes and Landforms*, *44*(1), 342–353. https://doi.org/10.1002/esp.4486

Lininger, K. B., Wohl, E., Rose, J. R., & Leisz, S. J. (2019). Significant Floodplain Soil Organic Carbon Storage Along a Large High-Latitude River and its Tributaries. *Geophysical Research Letters*, *46*(4), 2121–2129. https://doi.org/10.1029/2018GL080996

Lininger, Katherine B., & Wohl, E. (2019). Floodplain dynamics in North American permafrost regions under a warming climate and implications for organic carbon stocks: A review and synthesis. *Earth-Science Reviews*, *193*, 24–44. https://doi.org/10.1016/j.earscirev.2019.02.024

Livers, B., & Wohl, E. (2015). An evaluation of stream characteristics in glacial versus fluvial process domains in the Colorado Front Range. *Geomorphology*, *231*, 72–82. https://doi.org/10.1016/j.geomorph.2014.12.003

Livers, B., & Wohl, E. (2016). Sources and interpretation of channel complexity in forested subalpine streams of the Southern Rocky Mountains: CHANNEL COMPLEXITY IN FORESTED STREAMS. *Water Resources Research*, *52*(5), 3910–3929. https://doi.org/10.1002/2015WR018306

Livers, B., Wohl, E., Jackson, K. J., & Sutfin, N. A. (2018). Historical land use as a driver of alternative states for stream form and function in forested mountain watersheds of the Southern Rocky Mountains. *Earth Surface Processes and Landforms*, *43*(3), 669–684. https://doi.org/10.1002/esp.4275

Lynch, L. M., Machmuller, M. B., Boot, C. M., Covino, T. P., Rithner, C. D., Cotrufo, M. F., et al. (2019). Dissolved organic matter chemistry and transport along an Arctic tundra hillslope. *Global Biogeochemical Cycles*.

Lynch, L. M., Sutfin, N. A., Fegel, T. S., Boot, C. M., Covino, T. P., & Wallenstein, M. D. (2019). River channel connectivity shifts metabolite composition and dissolved organic matter chemistry. *Nature Communications*, *10*(1), 459. https://doi.org/10.1038/s41467-019-08406-8

Manga, M., & Kirchner, J. W. (2000). Stress partitioning in streams by large woody debris. *Water Resources Research*, *36*(8), 2373–2379. https://doi.org/10.1029/2000WR900153

McCain, J. F., & Shroba, R. R. (1979). *Storm and flood of July 31-August 1, 1976, in the Big Thompson River and Cache la Poudre River basins, Larimer and Weld Counties, Colorado* (USGS Numbered Series No. 1115- A,B). U.S. Govt. Print. Off.,. Retrieved from http://pubs.er.usgs.gov/publication/pp1115AB

Montgomery, D. R., & Abbe, T. B. (2006). Influence of logjam-formed hard points on the formation of valley-bottom landforms in an old-growth forest valley, Queets River, Washington, USA. *Quaternary Research*, *65*(1), 147–155. https://doi.org/10.1016/j.yqres.2005.10.003

Montgomery, D. R., & Buffington, J. M. (1997). Channel-reach morphology in mountain drainage basins. *GSA Bulletin*, *109*(5), 596–611. https://doi.org/10.1130/0016-7606(1997)109<0596:CRMIMD>2.3.CO;2

Omengo, F. O., Geeraert, N., Bouillon, S., & Govers, G. (2018). Deposition and fate of organic carbon in floodplains along a tropical semiarid lowland river (Tana River, Kenya). *Journal of Geophysical Research: Biogeosciences*, 1131–1143. https://doi.org/10.1002/2015JG003288@10.1002/(ISSN)2169-8961.CNFLOI1

Oost, K. V., Verstraeten, G., Doetterl, S., Notebaert, B., Wiaux, F., Broothaerts, N., & Six, J. (2012). Legacy of human-induced C erosion and burial on soil–atmosphere C exchange. *Proceedings of the National Academy of Sciences*, *109*(47), 19492–19497. https://doi.org/10.1073/pnas.1211162109

Parker, G. (1990). Surface-based bedload transport relation for gravel rivers. *Journal of Hydraulic Research*, *28*(4), 417–436. https://doi.org/10.1080/00221689009499058

Polvi, L. E., & Wohl, E. (2012). The beaver meadow complex revisited – the role of beavers in post-glacial floodplain development. *Earth Surface Processes and Landforms*, *37*(3), 332–346. https://doi.org/10.1002/esp.2261

Polvi, L. E., & Wohl, E. (2013). Biotic Drivers of Stream PlanformImplications for Understanding the Past and Restoring the Future. *BioScience*, *63*(6), 439–452. https://doi.org/10.1525/bio.2013.63.6.6

Polvi, L. E., Wohl, E. E., & Merritt, D. M. (2011). Geomorphic and process domain controls on riparian zones in the Colorado Front Range. *Geomorphology*, *125*(4), 504–516. https://doi.org/10.1016/j.geomorph.2010.10.012

Quinn, J. M., Phillips, N. R., & Parkyn, S. M. (2007). Factors influencing retention of coarse particulate organic matter in streams. *Earth Surface Processes and Landforms*, *32*(8), 1186–1203. https://doi.org/10.1002/esp.1547

R Core Team. (2017). *R: A language and environment for statistical computing*. Vienna, Austria: R Foundation for Statistical Computing. Retrieved from http://www.R-project.org/

Santín, C., Doerr, S. H., Preston, C. M., & González-Rodríguez, G. (2015). Pyrogenic organic matter production from wildfires: a missing sink in the global carbon cycle. *Global Change Biology*, *21*(4), 1621–1633. https://doi.org/10.1111/gcb.12800

Scott, D. N., & Wohl, E. E. (2018). Geomorphic regulation of floodplain soil organic carbon concentration in watersheds of the Rocky and Cascade Mountains, USA. *Earth Surface Dynamics*, *6*(4), 1101–1114. https://doi.org/10.5194/esurf-6-1101-2018

Sear, D. A., Millington, C. E., Kitts, D. R., & Jeffries, R. (2010). Logjam controls on channel:floodplain interactions in wooded catchments and their role in the formation of multi-channel patterns. *Geomorphology*, *116*(3), 305–319. https://doi.org/10.1016/j.geomorph.2009.11.022

Simon, A., & Collison, A. J. C. (2002). Quantifying the mechanical and hydrologic effects of riparian vegetation on streambank stability. *Earth Surface Processes and Landforms*, *27*(5), 527–546. https://doi.org/10.1002/esp.325

Stegen, J. C., Fredrickson, J. K., Wilkins, M. J., Konopka, A. E., Nelson, W. C., Arntzen, E. V., et al. (2016). Groundwater–surface water mixing shifts ecological assembly processes and stimulates organic carbon turnover. *Nature Communications*, *7*(1), 11237. https://doi.org/10.1038/ncomms11237

Stewart, I. T. (2009). Changes in snowpack and snowmelt runoff for key mountain regions. *Hydrological Processes*, *23*(1), 78–94. https://doi.org/10.1002/hyp.7128

Sutfin, N. (2020). Floodplain organic carbon storage along streams in the Colorado Front Range, U.S.A. https://doi.org/10.6084/m9.figshare.12014586.v1

Sutfin, N. A., & Wohl, E. (2017). Substantial soil organic carbon retention along floodplains of mountain streams. *Journal of Geophysical Research: Earth Surface*, *122*(7), 1325–1338. https://doi.org/10.1002/2016JF004004

Sutfin, N. A., & Wohl, E. (2019). Elevational differences in hydrogeomorphic disturbance regime influence sediment residence times within mountain river corridors. *Nature Communications*, *10*(1), 2221. https://doi.org/10.1038/s41467-019-09864-w

Sutfin, N. A., Wohl, E. E., & Dwire, K. A. (2016). Banking carbon: a review of organic carbon storage and physical factors influencing retention in floodplains and riparian ecosystems. *Earth Surface Processes and Landforms*, *41*(1), 38–60. https://doi.org/10.1002/esp.3857

Tranvik, L. J., Downing, J. A., Cotner, J. B., Loiselle, S. A., Striegl, R. G., Ballatore, T. J., et al. (2009). Lakes and reservoirs as regulators of carbon cycling and climate. *Limnology and Oceanography*, *54*(6part2), 2298–2314. https://doi.org/10.4319/lo.2009.54.6_part_2.2298

Trenberth, K. E., Dai, A., Schrier, G. van der, Jones, P. D., Barichivich, J., Briffa, K. R., & Sheffield, J. (2014). Global warming and changes in drought. *Nature Climate Change*, *4*(1), 17–22. https://doi.org/10.1038/nclimate2067

Vannote, R. L., Minshall, G. W., Cummins, K. W., Sedell, J. R., & Cushing, C. E. (1980). The River Continuum Concept. *Canadian Journal of Fisheries and Aquatic Sciences*, *37*(1), 130–137. https://doi.org/10.1139/f80-017

Veblen, T. T., & Donnegan, J. (2005). *Historical Range of Variability for Forest Vegetation of the National Forests of the Colorado Front Range* (p. 154). Golden, CO: USDA Forest Service, Rocky Mountain Region.

Venarsky, M. P., Walters, D. M., Hall, R. O., Livers, B., & Wohl, E. (2018). Shifting stream planform state decreases stream productivity yet increases riparian animal production. *Oecologia*, *187*(1), 167–180. https://doi.org/10.1007/s00442-018-4106-6

Wang, Z., Hoffmann, T., Six, J., Kaplan, J. O., Govers, G., Doetterl, S., & Van Oost, K. (2017). Human-induced erosion has offset one-third of carbon emissions from land cover change. *Nature Climate Change*, *7*(5), 345–349. https://doi.org/10.1038/nclimate3263

Ward, J. V., Tockner, K., Edwards, P. J., Kollmann, J., Bretschko, G., Gurnell, A. M., et al. (1999). A reference river system for the Alps: the 'Fiume Tagliamento.' *Regulated Rivers: Research & Management*, *15*(1-3), 63–75. https://doi.org/10.1002/(SICI)1099-1646(199901/06)15:1/3<63::AID-RRR538>3.0.CO;2-F

Weishaar, J. L., Aiken, G. R., Bergamaschi, B. A., Fram, M. S., Fujii, R., & Mopper, K. (2003). Evaluation of Specific Ultraviolet Absorbance as an Indicator of the Chemical Composition and Reactivity of Dissolved Organic Carbon. *Environmental Science & Technology*, *37*(20), 4702–4708. https://doi.org/10.1021/es030360x

Westerling, A. L., Hidalgo, H. G., Cayan, D. R., & Swetnam, T. W. (2006). Warming and Earlier Spring Increase Western U.S. Forest Wildfire Activity. *Science*, *313*(5789), 940–943. https://doi.org/10.1126/science.1128834

978 Wohl, E. (2008). The effect of bedrock jointing on the formation of straths in the Cache la Poudre River
979 drainage, Colorado Front Range. *Journal of Geophysical Research: Earth Surface*, *113*(F1).
980 https://doi.org/10.1029/2007JF000817
981 Wohl, E. (2013). Landscape-scale carbon storage associated with beaver dams. *Geophysical Research*
982 *Letters*, *40*(14), 3631–3636. https://doi.org/10.1002/grl.50710
983 Wohl, E. (2014). A legacy of absence: Wood removal in US rivers. *Progress in Physical Geography: Earth*
984 *and Environment*, *38*(5), 637–663. https://doi.org/10.1177/0309133314548091
985 Wohl, E., & Scott, D. N. (2017). Wood and sediment storage and dynamics in river corridors. *Earth*
986 *Surface Processes and Landforms*, *42*(1), 5–23. https://doi.org/10.1002/esp.3909
987 Wohl, E., Dwire, K., Sutfin, N., Polvi, L., & Bazan, R. (2012). Mechanisms of carbon storage in
988 mountainous headwater rivers. *Nature Communications; London*, *3*, 1263.
989 http://dx.doi.org/10.1038/ncomms2274
990 Wohl, E., Hall, R. O., Lininger, K. B., Sutfin, N. A., & Walters, D. M. (2017). Carbon dynamics of river
991 corridors and the effects of human alterations. *Ecological Monographs*, *87*(3), 379–409.
992 https://doi.org/10.1002/ecm.1261
993 Wohl, E., Lininger, K. B., & Scott, D. N. (2017). River beads as a conceptual framework for building carbon
994 storage and resilience to extreme climate events into river management. *Biogeochemistry*, 1–
995 19. https://doi.org/10.1007/s10533-017-0397-7
996 Wohl, E., Lininger, K. B., Rathburn, S. L., & Sutfin, N. A. (2020). How geomorphic context governs the
997 influence of wildfire on floodplain organic carbon in fire-prone environments of the western
998 United States. *Earth Surface Processes and Landforms*, *45*(1), 38–55.
999 https://doi.org/10.1002/esp.4680
1000